Feasibility of a Photovoltaic-Thermoelectric Generator: Performance Analysis and Simulation Results

Published Source
F. Attivissimo, A. Di Nisio, A.M.L. Lanzolla, M. Paul "Feasibility of a Photovoltaic–Thermoelectric Generator: Performance Analysis and Simulation Results "
IEEE Transactions on Instrumentation and Measurement vol. 64, no. 5, pp. 1158- 1169, May 2015, doi: 10.1109/TIM.2015.2410353

Feasibility of a Photovoltaic-thermoelectric generator: Performance Analysis and Simulation Results

F. Attivissimo[1], IEEE Member, A. Di Nisio[1], IEEE Member, A. M. L. Lanzolla[1], IEEE Member and M. Paul[2]

[1]Department of Electrical and Information Engineering (DEI)
Polytechnic of Bari
Via E. Orabona 4, 70125 Bari Italy
[attivissimo, dinisio, lanzolla]@misure.poliba.it

[2]School of Engineering
University of Glasgow,
Glasgow G12 8QQ, UK
Manosh.Paul@glasgow.ac.uk

Abstract – The paper describes a theoretical approach to evaluate the performance of a hybrid solar system made with photovoltaic cells and thermoelectric modules. After a brief treatment of the integrated system, energy conversion and performance parameters are evaluated through numerical simulations depending on the global radiation and temperature distribution obtained by the Joint Research Centre of the European Commission and of the National Renewable Energy Laboratory. The contributes of thermoelectric module to total energy seems significant in southern Europe towns and less substantial when the locations considered are very distant from the equator and show the possibility of using thermoelectric devices for energy production.

Keywords – *Solar cells, photovoltaic solar energy, photovoltaic cell model, thermoelectric conversion, thermoelectric module model, conversion efficiency***.**

TERMINOLOGY

α	temperature coefficient for short-circuit current [A/K]
A_p	photovoltaic module surface [m^2]
A_t	thermo-element area [mm^2]
E_g	energy band gap [eV]
ε_{STC}	efficiency at Standard Test Conditions (STC)
ε	efficiency
ε_{PVTE}	efficiency of photovoltaic- thermoelectric module
ε_{TE}	efficiency of thermoelectric module ε_{PV} efficiency of photovoltaic module

FF	fill factor
G_{ref}	irradiance at STC [W/m^2]
G	irradiance on horizontal surface [W/m^2]
I	thermo-module current [A]
I_L	photo-generated current [A]
I_{OD1}, I_{OD2}	reverse saturation diode current [A]
I_{sc}	short-circuit current in STC [A]
I_{mp}	current at maximum power point [A]
k	Boltzmann’s constant [J/K]
h_t	thermo-element length [mm]
h_c	copper contact length [mm]
h_p	ceramic element length [mm]
h_s	ratio between contact superficial electric resistivity and the thermo-element electric resistivity [mm]
A_t	thermo-element area [mm^2]
n_1, n_2	ideality factor
s	thermocouple Seebeck coefficient [V/K]
λ	thermocouple thermal conductivity [W/mm K]
ρ	thermocouple electric resistivity [Ω mm]
ρ_c	contact superficial resistivity [Ω mm^2]
λ_p	ceramic isolator thermal conductivity [W/mm K]
P_n	nominal power of the photovoltaic of the solar generator [W]
$P_{out_{PV}}$	electrical power output of the PV module [W]
$P_{out_{TE}}$	electrical power output of the TE module [W]
$P_{out_{PVTE}}$	electrical power output of the PV/TE system [W]
Q	rate of heat liberated by the thermoelectric module [W]
Q_{TE}	rate of heat liberated by the thermocouple [W]
R_{in}	thermo-module resistance [Ω]
R_L	electric load resistance [Ω]
R_S	series resistance [Ω]
R_{Sh}	shunt resistance [Ω]
T_{ref}	cell temperature at STC [K]
T_{max}	maximum photovoltaic module temperature [K]
T_{amb}	ambient temperature [K]
T_m	operating temperature [K]
T_{avg}	average temperature [K]
T'_h	hot junction temperature [K]
T'_c	cold junction temperature [K]
T	cell temperature [K]
V	voltage [V]

V_o thermoelectric generator open-circuit voltage [V]
V_{oc} open-circuit voltage in STC [V]
V_T thermal voltage [V]
V_{mp} voltage at maximum power point [V]

I. INTRODUCTION

In recent years, the fast development and the growing demand of comfort is rising the energy consumption; surging oil and gas consumption and increasing environmental awareness has prompted more and more sustainable development [1]; originally born as a problem of ethics and morality, the development of the alternative energy sources became a pressing requirement since the global pollution problem has become relevant. In the last decade, photovoltaic (PV) technology has attracted strong interest of the industry and of many researchers [2]. Research on solar cell was made since 1960 and different technologies have been proposed in order to reduce the material and to increase the production capacity.

At present silicon modules represent the leading PV technology thanks to both their capability to provide high efficiency and the great availability of silicon material on the earth. In particular monocrystalline solar cells offer highest efficiency with more that 20% [3]. Two alternative typologies developed to reduce the cost in PV modules production are *(i)* the polycrystalline silicon which provides worse performance in terms of efficiency (13-16%) and *(ii)* the amorphous silicon which offer low efficiency (6-9%) but is less affected by high temperatures and shading.

With respect to the PV cells based on crystalline silicon, thin film technology is less expensive since it uses few materials and less manufacturing process. Depending on the technology, thin-film module prototypes have reached efficiencies between 7–13% [4], [5].

Despite PV is considered a commercially mature technology, the efficiency of the PV plants is still quite low, therefore in the best of cases about 80% of the potential energy available would be wasted. On the other hand, this technology reduces continuously its cost and requires technical advance and new research for efficiency increment [6], [7]. Therefore, many researches have focused on the reduction of the losses that affect solar panels such as losses caused by the sunlight, the conditioning circuit required, the energy storage system, the Joule effect and so on [8], [9].

In order to reduce these effects, researchers are focusing on two strategies: to develop new materials or to try recovering part of the energy lost as heat by Joule effect [10], [11]. Therefore, nowadays, panel's manufacturers have high interest in combining thermoelectric

(TE) and photovoltaic effects to obtain higher performance. The low efficiency of TE energy conversion has limited the use of TE in electric power generation but this technology is evolving to a higher level of performance [12]. On the other hand, TE generators are preferred to recovery large amounts of waste heat or when the thermal input is free. Common applications of this conversion are the energy recovery from the waste heat of electronic hot components or cooling and heating PV elements in order to increase its efficiency or powering autonomous sensors [13]-[16]. Latest applications of the TE conversion are addressed to PV systems as active cooling or additional power generation of PV panels both using the difference between the ambient temperature and high panel temperature caused by the solar irradiation. The performance of a TE module is represented by the so-called figure of merit (Z) of the TE material or by the dimensionless ZT_{avg} product [23], [24], being T_{avg} the average temperature of the TE module.

The figure of merit Z represents the conversion efficiency from thermal energy into electrical energy and is strongly TE materials dependent. To optimize this parameter a large Seebeck coefficient, high electrical conductivity and low thermal conductivity are required.

For near room temperature applications (300 K) bismuth chalcogenides such as Bi_2Te_3 or Bi_2Se_3 materials provides the greatest figure of merit; for mid temperatures (500-900 K) Magnesium group IV compounds are mainly preferred; instead for high temperatures silicon – germanium materials are typically used.

Typical values of ZT_{avg} range in [0.7-0.8] but materials currently available reach values of 1; ZT_{avg} goes beyond of 1.2 for nanostructured bismuth antimony telluride bulk alloys [25]. In TABLE I. standard values of figure of merit are listed for different thermoelectric materials.

A hybrid photovoltaic-thermoelectric (PVTE) system can be found in many configurations where the two modules can be separated or integrated. No integrated hybrid systems are retrievable in cars [27], in some systems of harvesting energy, in particular types of telecommunication applications [28]; in some cases, these two modules are separated requiring an electronic controller [29], [30]. The integrated panels combine these devices in order to optimize the performance of both sources [9]. In this paper the performances of an integrated PVTE system was analyzed varying the site and using solar irradiation, temperature and sunshine hours available on solar energy database of the European Joint Research Centre [31]. Using databases of irradiance, temperature and other climatic parameters the authors evaluate the annual performance of the PVTE system at different European sites analyzing the additional TE power; the consistency of data used, with a ten years coverage over most of the regions considered, assure the reliability of the obtained results and can provide information to investors, authorities and renewable energy market.

For this aim, first the theory of PV and TE conversion is shortly summarized; then the model and the estimation algorithms of both photovoltaic and thermoelectric modules are implemented with Matlab functions and verified by simulating commercial modules.

TABLE I. FIGURE OF MERIT FOR DIFFERENT THERMOELECTRIC MATERIALS [26]

Thermoelectric material	**Material name**	**Manufacturing type**	**ZT_{avg}**	**Scenario Temperature**
Chalcogenides	Bi_2Te_3	bulk	0.74	low
	$Bi_{0.52}Sb_{1.48}Te_3$	bulk	1.05	low
	$Bi_{0.52}Sb_{1.48}Te_3$	nanobulk	0.52	low
	$Na_{0.0283}Pb_{0.945}Te_{0.9733}$	nanobulk	1.45	high
Silicon-germanium	SiGe	bulk	0.3	high
	$Si_{80}Ge_{20}$	banowire	0.53	high
	SiGe	nanobulk	0.22	low
Skutterudites	$CeFe_4Sb_{12}$	bulk	0.77	high
	$Yb_{0.2}In_{0.2}Co_4Sb_{12}$	bulk	0.93	high
	$Ca_{0.18}Co_{3.97}Ni_{0.03}Sb_{12.40}$	bulk	0.77	high
Oxides	$Ca_{2.4}Bi_{0.3}Na_{0.3}Co_4O_9$	bulk	0.13	high

II. THE MODEL

A. SYSTEM LAYOUT AND ASSUMPTIONS

A schematic representation of the PVTE system is reported in Fig.1 where the two blocks represent the PV and the TE modules; the thermal energy generated in the first block is converted to electricity by the second block. These elements can be reasonably considered separately, since the effects that lead to the generation of current can be considered independent of each other; indeed, even if the TE module is posteriorly integrated into the solar panel, and it exploits the temperature of the rear of the panel itself, this phenomenon affects the solar cell performance in a reasonably negligible way.

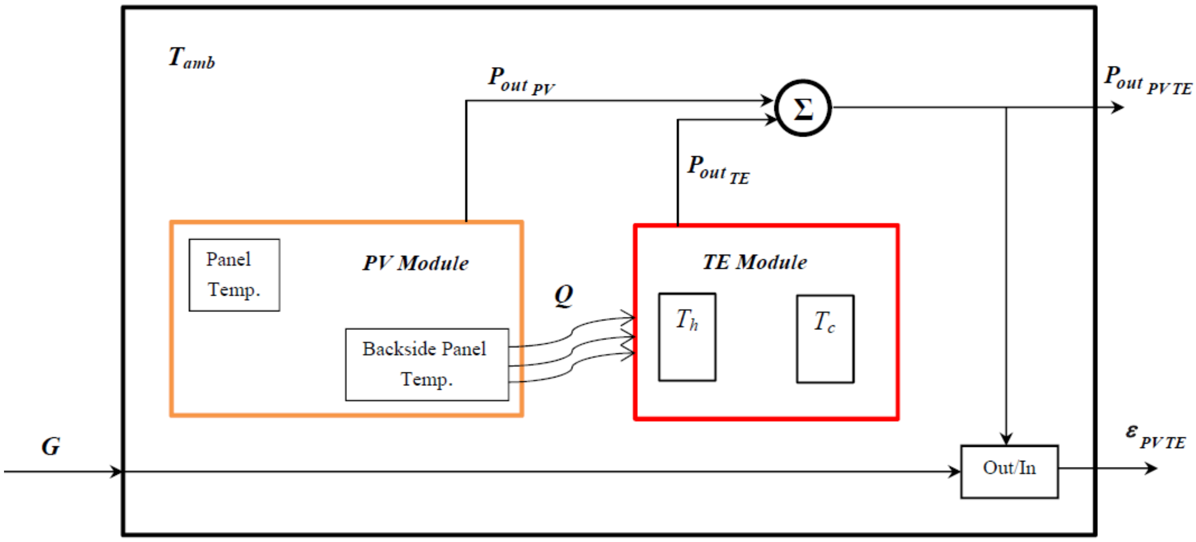

Fig.1 - *PVTE hybrid system representation*

The system operates at room temperature having as input the solar radiation and as output the total electric power generated by the system. At high solar irradiance the PV module temperature (T_{max}) can reach 50-60 °C and differs from room temperature by about 30°- 40° C (ΔT). These values depend on the site, the type of the integration and of the period of year considered. To calculate the PV panel temperature (T), which strongly depends on the incident light, the working conditions and the installation conditions, the following relation was used [32]:

$$T = T_{amb} + c \cdot G \qquad (1)$$

being G [W/m^2] the irradiance and c [K· m^2/W] a coefficient, known as the Ross coefficient, which depends on the installation conditions of the PV panel. The values of c are 0.058 K· m^2/W for roof PV panels integrated, 0.036 K· m^2/W for top of roof with small roof-module distance (<10 cm), 0.027 K· m^2/W for on top of roof with large roof-module distance (> 10cm), and 0.020 K· m^2/W for free-standing.

In TABLE II. the obtained values for the six considered sites [31] are listed, where $T_{\max}$ represents the maximum value of the panel temperature and ΔT is the difference between $T_{\max}$ and T_{amb} at different c for each town considered.

TABLE II. MAX VALUES OF MODULE TEMPERATURE AND TEMPERATURE DIFFERENCE AT DIFFERENT SITES FOR DIFFERENT PV INSTALLATION CONDITIONS

City	T_{max} [°C]				ΔT [°C]			
	c=0.058 K·m²/W	c =0.036 K·m²/W	c =0.027 K·m²/W	c =0.020 K·m²/W	c=0.058 K·m²/W	c =0.036 K·m²/W	c =0.027 K·m²/W	c =0.020 K·m²/W
Pachino (Sicily)	60	48	43	39	32	20	15	11
Taranto	58	46	41	38	31	19	14	11
Rome	56	45	40	36	30	19	14	10
Turin	50	41	37	34	26	16	12	9
Glasgow	32	26	23	22	16	10	7	5
Stockholm	37	30	28	25	18	11	8	6

The performance of the combined system should be given in terms of both generated electric power and overall system efficiency by highlighting their dependence on environmental conditions, such as temperature and radiation, and on physical properties of the used material.

Starting from these considerations the principle of superposition is therefore usable; then the generated electrical power of the overall system will be the sum of the electric powers generated by both modules. Under this assumption the overall efficiency of the system can be calculated as the ratio between the sum of the generated electric powers by each module, and the power of the input system, i.e. the solar radiation available to the PV module. In this case, both the front face temperature (T) and operating temperature of TE (T_m) will determine the PV and the TE module performance, respectively. Precisely, the temperature of the cells within the PV module (T) will depend on the ambient temperature (T_{amb}) and on the incident solar radiation flux (G); the operating TE temperature (T_m) will depend on rear panel temperature (T_h) and on the ambient temperature (T_{amb}). It is useful to note that there is a heat flow (Q) going from the PV to the TE module which is dissipated through the latter. Finally, in order to preserve the energy balance, the following losses should be considered:

- transformation losses due to conditioning circuits of the PV module (there are in fact inverter and other circuitries), which are not included in the model;
- losses due to the Joule effect in the PV module;
- losses due to the Joule effect in the TE module;
- losses due to dispersion currents;
- convection losses.

.

B. PV MATHEMATICAL MODEL

The simplest equivalent circuit of a PV cell consists of p-n junctions with a current generator current having intensity dependent on the incident radiation power:

$$I_{\mathrm{L}}\left(T,G\right)=I_{\mathrm{SC}}\left(T_{ref},G_{ref}\right)\frac{G}{G_{ref}}\left[1+\alpha\left(T-T_{ref}\right)\right] \quad (2)$$

where the parameter T points out the influence of the temperature on the solar cell. Both simulation and characterization of PV cells require parametric estimation of the model's parameters and many works are dedicated to this issue [33]; in [34] and an equivalent circuit with its parameters evaluation is presented, whereas in [35] an equivalent circuit based on double-diode representation is used. The mathematical model uses a current source having intensity proportional to the incident radiance and two diodes simulating diffusion and recombination processes. This accurate model highlights different physical characteristics which are independent from each other:

$$I=I_{\mathrm{L}}-I_{\mathrm{0D1}}\left[\mathrm{e}^{\frac{\left(V+R_{\mathrm{S}}\cdot I\right)}{\mathrm{V_T}\cdot\mathrm{n_1}}}-1\right]-I_{\mathrm{0D2}}\left[\mathrm{e}^{\frac{\left(V+R_{\mathrm{S}}\cdot I\right)}{\mathrm{V_T}\cdot\mathrm{n_2}}}-1\right]-\frac{V+R_{\mathrm{S}}\cdot I}{R_{Sh}} \quad (3)$$

where:

- $V_T=k\cdot T/q$
- q is the electron charge ($1.602\cdot10^{-19}$ C) and k the Boltzmann's constant ($1.38\cdot10^{-23}$ J/K);
- T is the absolute temperature (K) of the p-n junction
- I_{0D1} and I_{0D2} are the reverse saturation currents of the two diodes;
- n_1 and n_2 are the diodes ideality factors;
- R_s is the equivalent series resistance of the cell and R_{Sh} is the equivalent shunt resistance.

The saturation currents in model (3) depend on the intrinsic characteristics of the PV cell, which in turn depend on several physical parameters that are not usually available for the commercial PV arrays. The diode ideality factors values may be arbitrarily chosen but generally the initial values $n_1=1$ and $n_2=2$ can be selected in order to identify the model. A right estimation of these six parameters would be obtained by best fitting the model with a real panel. In Fig.2 the first diode represents the recombination current in the almost-neutral regions, while the second one represents recombination in the depletion region. In the same figure, R_S is the series resistance including the silicon wafer, the contact resistance and, also, the circuital resistance derived from connections to the terminals and thus, materially, represents losses by Joule effect. R_{sh} is the parallel resistance deriving from leakage currents at the solar cell edges and from the inhomogeneity of the surface's; it represents the losses due to leakage current towards ground. Both resistors make the characteristic curve less "rectangularly shaped" and they reduce the maximum output power. In an ideal solar cell, obviously the resistance values of R_S and R_{sh} should theoretically be zero and infinity respectively an assumption often used in the analysis and characterization of the panels.

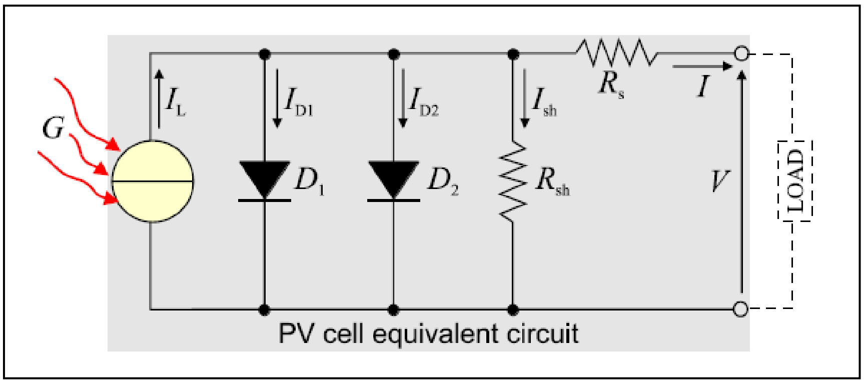

Fig.2 - *Two diodes equivalent circuit of a PV cell*

The extension of the model to a PV panel and a parallel string produces the equations [36]:

$$I_{\text{module}} = N_{\text{p}} \cdot I; V_{\text{module}} = N_{\text{s}} \cdot V$$
$$R_{\text{s module}} = R_{\text{s}} \cdot N_{\text{s}} / N_{\text{p}}; R_{\text{sh module}} = R_{\text{sh}} \cdot N_{\text{s}} / N_{\text{p}} \quad (4)$$

where a string is made of N_s cells in series, and a module is composed by N_p strings in parallel with the hypothesis that all the cells are identical and are subjected to the same radiance and temperature. This kind of model, known in the literature as *seven-parameters model* (I_L, I_{OD1}, I_{OD2}, n_1, n_2, R_S, R_{sh}), was already analysed by the authors using the Newton-Raphson method and its applicability to different plants has been verified [37].

C. TE MATHEMATICAL MODEL AND ITS VERIFICATION

The fundamental element of a TE module is the thermocouple which is realized with two legs of a different doped semiconductor material; they are made of n-type and p-type doped semiconductor doped and are connected to each other by a metal plate usually made of copper.

In Fig.3 a generic TE module with N_{TE} thermocouples connected electrically in series and thermally in parallel is represented where h_p is the ceramic plate length, h_t and A_t are the length and the cross-sectional area of the thermo-elements and h_c represents the copper contact length.

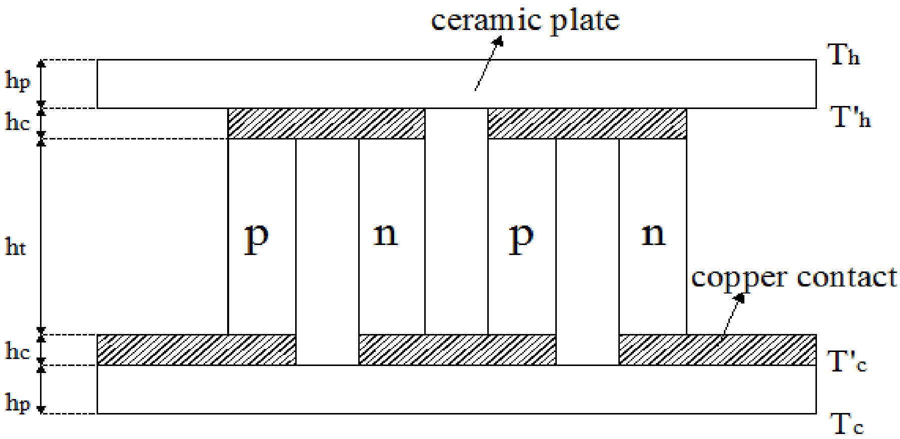

Fig.3 – *Basic structure of a TE module*

The thermal power extracted by a TE module is the result of the Peltier, Joule and Fourier effects which model this phenomenon by means of the Seebeck coefficient *s*, the electrical resistivity ρ and the thermal conductance λ of the material and of thermo-elements geometry as function of both hot-side T_h and cold-side T_c temperatures [38]:

$$Q_{TE} = N_{TE}\left[\lambda \frac{A_t}{h_t}\left(T_h - T_c\right) + s \cdot T_h \cdot I - \frac{1}{2} R \cdot I^2\right] \tag{5}$$

being *I* the thermo-module current and $R = \rho \cdot h_t / A_t$. Equation (5) is a simplified model of a TE module which consists of two semiconductor thermo-elements connected by conducting copper strips. A more accurate and realistic model requires to consider the thermal and electrical contact resistances between the thermo-elements and the ceramic plates. Precisely, the effect associated with ceramic layers, reduces the effective temperature difference across the two ends of the thermocouple according to:

$$\Delta T = T'_h - T'_c = \frac{T_h - T_c}{\left(1 + 2\dfrac{\lambda \cdot h_p}{\lambda_p \cdot h_t}\right)} \tag{6}$$

where the effects related to the connected load should be considered. Really, if a resistive load is connected across the TE module terminals, an electrical current depending on the resistor value will flow in the load; low resistance values will produce an increment of the current and as a result the cooling of the hot junction and heating of the cold junction. The reduction of ΔT caused by this effect is dependent on the operating temperature and on the thermoelectric module properties and can be generally neglected.

Similarly, accounting for the electrical contact's contribution R_c, the total electrical resistance of TE module can be expressed as:

$$R_{TE} = R + R_c = \frac{\rho \cdot h_t}{A_t} + 2\frac{\rho_c}{A_t} = \frac{\rho\left(2 \cdot h_s + h_t\right)}{A_t} \tag{7}$$

being ρ_c the contact superficial resistivity and putting $h_s = \rho_c / \rho$. Combining (5), (6) and (7) a more accurate expression of thermal power extracted by a TE module is obtained:

$$Q_{TE} = N_{TE}\left[\lambda \frac{A_t}{h_t}\left(T'_h - T_c'\right) + s \cdot T'_h \cdot I - \frac{1}{2} R_{TE} \cdot I^2\right] \tag{8}$$

Considering m TE modules connected electrically in series and thermally in parallel, the expression:

$$Q = m \cdot Q_{TE} \tag{9}$$

takes into account the heat flow passing through the thermocouple in steady state calculated as the sum of these three effects.

The first term in (8) accounts the heat conduction relevant to the temperature difference, the second one is the result of Peltier effects and the third term is representative of the Joule heating effect. Under these hypotheses, the current I, flowing in the electric load R_L connected to the TE generator, is given by:

$$I = m\frac{V_{TE}}{R_{in} + R_L} = \frac{V_o}{R_{in} + R_L} \tag{10}$$

where R_{in} is the internal electrical resistance of the TE generator, given by

$$R_{in} = m \cdot R_{TE} \tag{11}$$

and $V_o = m \cdot V_{TE} = m \cdot s \cdot N_{TE}\left(T'_h - T'_c\right) = m \cdot s \cdot N_{TE}\dfrac{\left(T_h - T_c\right)}{\left(1 + 2\dfrac{\lambda \cdot h_p}{\lambda_p \cdot h_t}\right)}$ (12)

the open-circuit voltage. The electric output power of the overall system is then [39]:

$$P_{out_{TE}} = \frac{V_o^2 \cdot R_L}{\left(R_L + R_{in}\right)^2} \tag{13}$$

and varies with R_L having a maximum when the load resistance match the internal resistance. Therefore, the load resistance value affects both the power generation performance and the Peltier effect at the interface with a change of temperature across the module. Particularly, in the case $R_L = R_{in}$ the maximum power transfer is realized with a negligible Peltier contribution to temperature reduction.

The electrical quantities in (10)-(13) are defined in terms of three materials properties (s, ρ, λ) that usually are not provided by manufacturers and vary with operating temperature. Generally, every manufacturer specifies the TE module producing performance curves, performance specifications $(Q_{TE_{\max}}, I_{TE_{\max}}, V_{TE_{\max}}, \Delta T_{\max}, R_{TE})$ and some geometrical parameters. The parameters (s, ρ, λ) can be accurately determined using experimental setup or using some theoretical equations [24], [40], [41]. Alternatively, these TE coefficients can be modelled, supposing a uniform temperature along the side of the module and using the operating temperature $T_m = \left(T_c + T_h\right)/2$ of the TE, by means of a second-order polynomials equation [42] depending on the manufacturer:

$$\begin{aligned} s &= a\left(T_m - 23\right)^2 + b\left(T_m - 23\right) + c \\ \rho &= d\left(T_m - 23\right)^2 + e\left(T_m - 23\right) + f \\ \lambda &= g\left(T_m - 23\right)^2 + h\left(T_m - 23\right) + i \end{aligned} \tag{14}$$

with
$$\begin{aligned} &a = -9.90 \cdot 10^{-10} [V/K^3];\ b = 3.44 \cdot 10^{-7} [V/K^2];\ c = 2.11 \cdot 10^{-4} [V/K]; \\ &d = 6.28 \cdot 10^{-11} [\Omega \cdot mm/K^2]; e = 5.35 \cdot 10^{-8} [\Omega \cdot mm/K];\ f = 10.85 \cdot 10^{-6} \left[\Omega \cdot mm\right]; \\ &g = 41.30 \cdot 10^{-6} \left[W/(mm \cdot K^3)\right];\ h = -3.32 \cdot 10^{-3} \left[W/(mm \cdot K^2)\right];\ i = 1.66 \left[W/(mm \cdot K)\right]; \end{aligned}$$

.

where the values used are related to CP2-127-06 TE module [43]. The consistence of the values obtained throught (14) has been verified with Matlab simulations calculating the Seebeck coefficient *s*, the electrical resistivity ρ and the thermal conductance λ of the material on the basis the manufacturer's specifications $(Q_{TE_{\max}}, I_{TE_{\max}}, V_{TE_{\max}}, \Delta T_{\max}, R_{TE})$; to this aim, three TE modules have been considered, i.e. Tellurex C2-30-1503, Marlov RC-12-4 and

Kryotherm TB 127-1-1.0-1.3. They are designed for cooling and heating applications with geometrical, electrical and thermal parameters reported in TABLE III.

TABLE III. CHARACTERISTIC PARAMETERS OF THE CONSIDERED THERMOELECTRIC MODULES

Manufacturer	**Model**	**Length** [mm]	**Width** [mm]	**Thickness** [mm]	R_{TE} [Ω]	ΔT_{max} [K]	Q_{TEmax} [W]
Tellurex	C2-30-1503	30.00	30.00	3.70	3.85	341.15	34.1
Marlov	RC-12-4	29.97	29.97	3.43	3.20	339.15	36.0
Kryotherm	TB-127-1.0-1.3	30.00	30.00	3.60	3.20	342.15	34.5

In TABLE IV. the values of (s, ρ, λ) estimated for the three TE module are reported.

TABLE IV. s, ρ, λ OBTAINED BY FITTING MANUFACTURER'S SPECIFICATIONS

Manufacturer	**Model**	s [V/K]	ρ [Ω mm]	λ [W/mm K]
Tellurex	C2-30-1503	208.39e-6	10.07e-4	17.08e.3
Marlov	RC-12-4	209.24e-6	11.31e-4	16.07e.3
Kryotherm	TB-127-1.0-1.3	205.53e-6	10.06e-4	15.97e.3

The goodness of the model has been verified using the specifications of the CP2-127-06 TE module and comparing (see TABLE V. the results of (14) with the results obtained by using the model in [44], [45] for different values of temperature; T_c values are the average temperatures relevant to both coldest and the hottest month of the year and T_h values are the front panel tempearature evaluated through (1) considering the environmental parameters of the site (T_c, G) and PV panels installed on the top of roof with small roof-module distance ($c=0.036\ K{\cdot}m^2/W$). An in-depht analysis of the results shows that the maximum deviation of the figure of merit $Z = s^2/\rho\,\lambda$ between estimated using (14) and [44], [45] is less than 0.7%.

TABLE V. COMPARISON BETWEEN s, ρ, λ ESTIMATION BY (14) AND [44], [45] USING THE CP2-127-08 TE SPECIFICATIONS

City	T_c [°C]	T_h [°C]	s [V/K]	ρ [Ω mm]	λ [W/mm K]	s [V/K]	ρ [Ω mm]	λ [W/mm K]
			Eq. (14)			[44], [45]		
Pachino (Sicily)	13	29	210.21e-6	10.74e-4	16.66e.3	210.26e-6	10.75e-4	16.66e.3
	28	48	215.84e-6	11.64e-4	16.18e.3	215.89e-6	11.67e-4	16.19e.3
Taranto	10	23	208.62e-6	10.50e-4	16.82e.3	208.67e-6	10.51e-4	16.83e.3
	27	46	215.37e-6	11.56e-4	16.22e.3	215.41e-6	11.59e-4	16.22e.3

Rome	9	21	208.08e-6	10.42e-4	16.88e.3	208.13e-6	10.43e-4	16.89e.3
	26	45	215.05e-6	11.51e-4	16.24e.3	215.09e-6	11.53e-4	16.25e.3
Turin	5	17	206.63e-6	10.20e-4	17.05e.3	206.68e-6	10.22e-4	17.05e.3
	25	41	214.25e-6	11.38e-4	16.30e.3	214.29e-6	11.40e-4	16.31e.3
Glasgow	5	9	205.14e-6	9.98e-4	17.23e.3	205.19e-6	10.02e-4	17.23e.3
	16	26	210.21e-6	10.74e-4	16.66e.3	210.26e-6	10.75e-4	16.66e.3
Stockholm	-1	3	202.85e-6	9.64e-4	17.52e.3	202.90e-6	9.71e-4	17.52e.3
	19	30	211.41e-6	10.93e-4	16.54e.3	211.46e-6	10.94e-4	16.55e.3

Finally, substituting in (10) - (13) the parameters s, ρ,λ estimated throught (14) it is possible to obtain the electrical parameters of the TE module.

D. PVTE PERFORMANCE INDEXES

The mathematical model of the hybrid system is based on the integration of the PV cells with the TE modules previously described; the system combines radiation and thermal energy to produce electricity. In particular, the PV cells convert solar radiation into electricity whereas the TE modules transform the heat generated below the PV cells in electric power.

In this analysis it is assumed that the rear temperature of the panel almost equal to the temperature present on the front side of the panel itself and that the TE module posteriorly integrated into the PV panel with the hot junction at the same temperature of rear side of the panel and the cold junction at ambient temperature [14], [46], [47].

It is well known that when the PV module works at the maximum power point, its output power can be expressed as:

$$P_{out,max_{PV}} = I_{mp} \cdot V_{mp} \qquad (15)$$

where I_{mp} and V_{mp} are the current and the voltage calculated at the maximum power point, respectively, even if environmental conditions can produce performances variation especially in PV plants where several modules are connected in string [48].

As regards the PV module, the efficiency assessed under the universally recognized standard test conditions (STC), is expressed in terms of the open-circuit voltage and the short-circuit current, as:

$$\varepsilon_{PV_{STC\%}} = \frac{FF \cdot I_{sc} \cdot V_{oc}}{A_p \cdot G_{STC}} \cdot 100 = \frac{I_{mp} \cdot V_{mp}}{A_p \cdot G_{STC}} \cdot 100 \qquad (16)$$

where A_p and $FF = I_{mp} \cdot V_{mp} / I_{sc} \cdot V_{oc}$ are the area and fill factor of the PV panel, respectively. Under these assumptions, the efficiency of the PV module at a generic radiance (G) is expressed as:

$$\varepsilon_{PV\%} = \frac{I_{mp} \cdot V_{mp}}{A_p \cdot G} \cdot 100 \tag{17}$$

while, the final yield, useful to compare different PV systems at the same operating site, is expressed as:

$$Y_{PV} = \frac{E_{PV}}{P_n} \tag{18}$$

where E_{PV} is the average energy that the PV panel generates monthly or yearly and P_n is the nominal power of the solar generator. TE performance varies significately with TE materials, module geometry and contact properties; the maximum otput power depends on both the amount of input heat and of the load resistance R_L which should be as close as possible to the internal electrical resistance of the thermo-generator R_{in}. Moreover the conversion efficiency increases with temperature difference and thermo-element length [49]. In relation to R_{in}, the power output of the TE module increases with the number of the modules because the electric output power increases with "the square of *m*" while efficiency remains almost unchanged.

It could occur that when the current in the thermo-element increases, the component related to the Joule effect takes over on other energy components; this means a drastic performance reduction in terms of both efficiency and power. For this reason, when the TE module is forced to work under these conditions, it is preferred to increase *m*; obviously, this provides the physical limit for having no losses. However, where the space and the costs allow it, the use of multiple TE modules is advisable to increase the output power.

Finally, the TE global efficiency and the final yield can be expressed as:

$$\varepsilon_{TE} = \frac{P_{out_{TE}}}{Q} \tag{19}$$

In the proposed analysis m=37 TE modules integrated behind the PV panel have been considered. In this case the total generated power of the PVTE hybrid system is the sum of the power output of each system:

$$P_{out,max_{PVTE}} = P_{out,max_{PV}} + P_{out_{TE}} \tag{20}$$

with a conversion efficiency given by:

$$\varepsilon_{PVTE\%} = \frac{P_{out,max_{PV}} + P_{out_{TE}}}{G} \cdot 100 \quad (21)$$

Then, the energy generated by the PVTE hybrid system is calculated by summing the overall power at each single hour as:

$$E_{PVTE} = P_{out,max_{PVTE}} \cdot h \quad (22)$$

where *h* represents the hours of average radiance; so the final yield of the overall system performance is:

$$Y_{PVTE} = \frac{E_{PVTE}}{P_n} \quad (23)$$

according to IEC standard 61724 [50].

III. TEST PERFORMANCE AND RESULTS

The performance of the PVTE system was characterized considering global radiation data at different sites by evaluating power and energy generated, efficiency and final yield for PV, TE and integrated PVTE system.

The sites have been chosen to verify how performance varies when the irradiance and the temperature distributions reach higher values. The radiance (G), the sunshine hours (d_h) and the ambient temperature (T_{amb}) used in the model have been obtained by using the online database provided by the Joint Research Centre of the European Commission and of the National Renewable Energy Laboratory [31].

In order to have a global view of the performance of the system under consideration, the data for each month of the year have been downloaded. For every day of each month the system acquires the data at regular intervals of 15 minutes sunrises to sunset; for each acquisition time the algorithm produces a mean of several measurements. TABLE VI. shows the average data of global radiance, ambient temperature and hours of daily radiance for best tilt solar panel. Data highlight that the towns closer to the equator have higher radiance and temperature values with respect to northern one with very similar trends. Small differences show Glasgow and Stockholm; in fact, during the coldest months of the year in Glasgow the radiance and the temperature are higher than in Stockholm while in the warmer months it is the opposite. Finally, the average hours of radiance over a year shows that in the winter months, the cities farthest from the equator have shorter days with respect to those in southern Europe; vice versa in the summer months, the cities in northern Europe have longer days and hence more hours of sunlight

In [38] an inclination angle of 0° was considered in order to verify the system performance with same initial conditions. Now, using best tilt angle, best performance should be estimated for each considered site.

TABLE VI. GLOBAL IRRADIANCE, AVERAGE TEMPERATURE AND DAYLIGHT HOURS FOR THE CONSIDERED SITES

	Stockholm			*Glasgow*			*Turin*			*Rome*			*Taranto*			*Pachino (Sicily)*		
Month	G [W/m^2]	T_{amb} [°C]	d_h [h]	G [W/m^2]	T_{amb} [°C]	d_h [h]	G [W/m^2]	T_{amb} [°C]	d_h [h]	G [W/m^2]	T_{amb} [°C]	d_h [h]	G [W/m^2]	T_{amb} [°C]	d_h [h]	G [W/m^2]	T_{amb} [°C]	d_h [h]
Jan	98	-1,1	06:15	121	4,9	07:15	325	5,2	08:45	330	9,2	09:15	360	10,3	09:15	433	12,7	09:45
Feb	194	-0,8	08:45	187	5,4	09:15	436	7,3	09:45	409	9,9	10:15	417	10,6	10:15	490	13,0	10:15
Mar	253	1,3	11:15	259	6,8	11:15	441	10,9	11:45	426	11,9	11:45	444	12,3	11:45	497	14,4	11:45
Apr	303	6,2	14:15	310	8,6	13:30	411	13,5	13:15	446	14,4	12:45	459	15,1	12:45	508	16,5	12:45
May	352	11,1	16:00	313	11,6	15:30	402	18,6	14:15	449	19,6	14:15	458	20,4	14:15	497	21,0	13:45
Jun	300	16,0	17:30	276	14,2	16:30	403	22,7	15:00	460	23,8	14:45	468	24,7	14:45	496	25,3	14:15
Jul	309	19,2	17:00	273	16,1	16:00	445	24,6	14:30	509	26,0	14:15	507	27,3	14:15	541	27,8	13:45
Aug	293	19,1	14:45	263	16,2	14:30	437	24,0	13:45	524	26,0	13:15	527	27,0	13:15	546	28,0	13:15
Sep	269	14,4	12:15	242	14,3	12:15	437	24,0	13:45	478	22,1	12:15	481	23,0	12:15	517	24,8	12:15
Oct	196	8,8	09:45	186	11,0	10:15	354	15,8	10:45	424	18,9	10:45	448	19,6	10:45	506	21,9	10:45
Nov	127	3,7	07:15	159	7,7	07:45	302	9,9	09:15	363	14,1	09:15	367	15,0	09:45	461	17,8	09:45
Dec	61	0,2	05:45	113	4,9	06:45	333	6,0	08:15	331	10,5	08:45	383	11,7	08:45	437	14,4	09:15
Best Tilt [°]	41			38			39			35			34			33		
Azimut [°]	0			0			0			0			0			0		
Latitude	59°19'44" North			55°57'2" Nord			45°4'15" North			41°53'34" North			40°27'56" Nord			36°42'43" North		
Longitude	18°3'53" East			4°6'34" Ovest			7°41'8" East			12°28'57" East			17°14'52 Est			15°5'33" East		

The tests have been conducted according to the hypotheses of *i)* solar module subjected to uniform illumination without shadow zones, *ii)* equal rear and front panel temperature, *iii)* TE hot junction temperature equal to rear temperature of the PV, *iv)* TE cold junction temperature equal to the ambient temperature (by assuming that the system is not working with an additional cooling system). The PV panel front temperature is been calculated by equation (1) using the value 0.036 K·m^2/W for c and considering the monthly average data of temperature and global radiation for each location at different times of the day. It is worth to underline that there is a wide literature which analyses the correlation among temperature, weather conditions and material properties and then several models for cell temperature have been proposed as a function of the wind speed, solar radiation and ambient temperature in different implicit and explicit equations [52]. The performance of the method has also been verified using one PV panel and $m=37$ TE modules. The PV was a IP10P model by Istar Solar consisting of N_p = 2 parallel-connected strings each composed by N_s=36 series-connected polycrystalline silicon cells and provides a peak output of 10 W [53]; the dimensions of the panel is 310 x 210 mm and its specifications in STC are listed in TABLE VII. The TE module considered was a TGM 127-1.0-1.3 [54] composed by 127 thermocouples connected thermally in parallel and electrically in series; the dimensions of the module is 30 x 30 mm; the thermal and electrical parameters of TE are presented in TABLE VIII. The TE generator was obtained considering thirty-seven TE modules connected electrically in series and thermally in parallel so to cover about 2/3 of the rear side of the cells.

TABLE VII. IP10P SPECIFICATIONS IN STC

Symbol	***Parameter***	***Value***
P_M	*Maximum Power (MP)*	10 W
V_{MP}	*Voltage @MP*	17 V
I_{MP}	*Current @MP*	0.6 A
V_{OC}	*Open-circuit Voltage*	21,6 V
I_{SC}	*Short-circuit Current*	0.67 A
α	*Current temperature coefficient*	0.07 %/°C
β	*Voltage temperature coefficient*	-0.34 %/°C

TABLE VIII. TGM 127-1.0-1.3 PERFORMANCE

Symbol	***Parameter***	***Value***
ΔT_{max}	*Maximum Temperature Difference*	150 °C
T_c	*Cold end Temperature*	0° C
V_{TE}	*Voltage*	2.5 V
I_{TE}	*Current*	0.59 A
P_{OUTTE}	*Power*	21,6 V

In TABLE IX. annual power and energy have been reported for each site; the values are been obtained summing the monthly values of power and energy. The TE module is more performing and helpful in warmer countries and the latitude mainly affects the performance of the TE generator with respect to PV panel; in fact, the value of E_{PV} is halved moving from Pachino to Glasgow or Stockholm, whereas the E_{TE} is reduced by about 1/3.

TABLE IX. ANNUAL POWER AND ENERGY CALCULATED FOR SITES CONDIDERED

	P_{PV} [W]	P_{TE} [W]	P_{PVTE} [W]	E_{PV} [Wh]	E_{TE} [Wh]	E_{PVTE} [Wh]
Pachino (Sicily)	1.737	239	1.976	20.198	2.792	22.989
Taranto	1.584	199	1.704	18.889	2.323	21.211
Rome	1.540	184	1.724	18.148	2.208	20.355
Turin	1.442	153	1.595	17.031	1.862	18.893
Glasgow	852	54	906	10.612	721	11.332
Stockholm	875	60	934	11.344	840	12.185

These conclusions seem to be confirmed considering the effect of the power and energy produced by TE with respect to PVTE system where the TE module contributes to total energy from 12.2 % in Pachino to about 6.5 % in Glasgow and Stockholm (TABLE X.). It is worth to note that the TE generator sited in Stockholm, in a time frame of an year, has better performance compared to the same TE generator in Glasgow despite Stockholm is more to north of Glasgow. The final yield values reported in the same table, which represent the annual produced energy normalised to rated power, are useful to compare the performance of PVTE system for different configurations and sites. An in depth analysis of these data shows that the final yield decrease no more than 45% for PV and up to 70% for TE. Same performance can be achieved varying the number of thermo-modules. Other tests carried out with the thermo-modules, and not reported in the paper for sake of brevity, seem to confirm the exposed results.

TABLE X. FINAL YIELD, POWER AND ENERGY CALCULATED FOR THE CONSIDERED SITES

	P_{TE}/P_{PVTE}	E_{TE}/E_{PVTE}	Y_{FTE}	Y_{FPV}
Pachino (Sicily)	12,11	12,14	50,30	2016,84
Taranto	11,70	10,95	41,85	1864,30
Rome	10,65	10,85	39,78	1815,46
Turin	9,57	9,86	33,55	1702,95
Glasgow	5,98	6,36	12,99	1061,98
Stockholm	6,39	6,90	15,14	1133,83

Finally, in TABLE XI. the values of the relative deviation percentage between the PV system and the hybrid system PVTE (d_{PVTE}) calculated for each month of the year, are indicated.

The data highlight that d_{PVTE} ranges in the interval 7.78-16.08 for the cities of southern Europe.

TABLE XI. PERCENTAGE PERFORMANCE " PVTE /PV" DEVIATION

Month	Pachino (Sicily)	Taranto	Rome	Turin	Glasgow	Stockholm
Jan	11,69	9,16	8,51	8,39	3,85	2,31
Feb	12,90	10,80	10,37	11,16	4,91	4,48
Mar	13,37	11,93	11,26	11,33	6,21	6,08
Apr	13,79	15,55	12,09	10,62	7,50	7,54
May	14,05	12,89	12,50	10,67	8,37	9,44
Jun	14,03	13,64	13,19	10,98	7,05	8,22
Jul	15,70	14,48	14,82	12,51	7,23	8,17
Aug	16,08	14,97	14,93	12,06	6,59	7,76
Sep	15,03	13,61	13,64	12,06	6,07	7,25
Oct	13,90	12,50	11,35	9,73	5,17	4,79
Nov	12,55	10,00	9,41	7,78	4,43	3,63
Dec	11,75	9,92	8,55	8,22	4,18	0,98

The best performances are obtained in August in the Pachino city (green cell) even if the TE power contribution is considerable in each site in the spring and summer months. Lower performance are obtained in northern towns (Glasgow and Stockholm), especially in the winter months; this unfavourable phenomenon happens in the particularly cold months of January and December in the city of Stockholm (red cells). In the same table, cells in yellow highlight that the maximum values are obtained, in all the cities, in the month of July or August except in Glasgow and Stockholm in which they are obtained in May. Although the TE module enhances annual PV performance, the extra cost of this device should be balanced by the energy produced. TE devices price varies from manufactures to manufacturer and TE materials keeps changing on with changing times. So, new products to the market bring fluctuation in TE price. Commercial modules are available in many size and with different power; generally, the price reduces when the power increases and for large quantities. Typical costs for TE generating modules varies from 2.40 to 6.80 $/W, which is higher than normal solar price of 0.58-1.28 $/W [55]; so the global extra cost of about four-five times higher than PV module makes less attractive current TE technology for this application and requires new researches in order to increase the efficiency and reduce the cost of these devices. However, the results suggest that to obtain systems with good reliability and cost-effective the design of a PVTE system should be tailored to location, individual requirements and meteorological condition and that the optimal number of TE module is dependent on the resistance of PV panel, on the type of components used and on the environmental parameters of the site.

IV. CONCLUSIONS

In the paper a complete model to evaluate the performance of a PVTE hybrid system is proposed and verified by simulation results. The obtained results seem to shown that the PV module is the primary source of energy of the system, even if the TE contribution is significant in southern Europe towns and that best performance are obtained for the locations having high radiance and low ambient temperature. A detailed analysis of the results indicated that the TE module produce good performance in the spring and summer months assuring promising contribution of energy even if the load resistance, the meteorological conditions and site should be carefully considered. New further research in TE material seem to promise high values of the figure of merit Z so to increase the TE efficiency up to 50%.; under this assumption the TE technology would be a viable candidate for alternative power generation.

ACKNOWLEDGMENT

The paper has been written within the framework of the project “RES NOVAE - Reti, Edifici, Strade - Nuovi Obiettivi Virtuosi per l’Ambiente e l’Energia”. This project is supported by the Italian University and Research National Ministry research and competitiveness program that Italy is developing to promote “Smart Cities Communities and Social Innovation”. The authors would like to thank Eng. D. Passaghe for his valuable contribution.

REFERENCES

[1] A. Malik, E. Grohmann, Environmental Protection Strategies for Sustainable Development, Springer, 2012.

[2] B. Sørensen, Renewable Energy: Its Physics, Engineering, Use, Environmental Impacts, Economy, and Planning Aspect, Academic Press, 2011.

[3] V. V. Tyagi, N. A. A. Rahim, N. A. Rahim, J. A. L.Selvaraj, Progress in solar PV technology: Research and achievement, Renewable and Sustainable Energy Reviews, n. 20 , April 2013, pp. 443-461.

[4] B. Parida, S. Iniyan, Ranko Goic, A review of solar photovoltaic technologies, Renewable and Sustainable Energy Reviews n.15, April 2011, pp. 1625 -1636.

[5] A. Gaur, G.N. Tiwari, Performance of a-Si thin film PV modules with and without water flow: An experimental validation, Applied Energy, vol. 128, no. 1, September 2014, pp. 184-191.

[6] A. Carullo, S. Corbellini, A. Luoni, A. Neri, In situ calibration of heterogeneous acquisition systems: the monitoring system of a photovoltaic plant, IEEE Transactions on Instrument and Measurement, vol. 59, no. 5, April 2010, pp. 1098-1103.

[7] L. Cristaldi, M. Faifer, M. Rossi, S. Toscani, An Improved Model-Based Maximum Power Point Tracker for Photovoltaic Panels, IEEE Transactions on Instrument and Measurement, vol. 63, no. 1, Jannuary 2014, pp. 63-71.

[8] A. Luque, S. Hegedus, Handbook of Photovoltaic Science and Engineering, Wiley, 2003.

[9] M. M. M. Daud, N. B. M. Nor, T. I.brahim, Novel Hybrid Photovoltaic and Thermoelectric Panel, Proc. of International Power Engineering and Optimization Conference, Melaka, Malaysia, June 2012, pp. 269-274.

[10] M. Fuentes, G. Nonfuentes, J. Aguilera, D. L. Talavera, M. Castro, Application and Validation of Algebraic Methods to Predict the Behaviour of Crystalline Silicon PV Modules in Mediterranean Climates, Solar Energy, vol. 81, November 2007, pp. 1396-1408.

[11] W. G. J. H. M. Van Sark, Feasibility of Photovoltaic-Thermoelectric hybrid Modules, Applied Energy, vol. 88, August 2011, pp. 2785-2790.

[12] H. Sasaky, K. Takahashi, D. Inglis, M. Klons, A numerical Simulation of Thermoelectric Effects in Single-Junction Thermal Converters, IEEE Transactions on Instrumentation and Measurement, vol.48, no. 2, April 1999, pp. 408-411.

[13] S. Dalola, M. Ferrari, V. Ferrari, M. Guizzetti, D. Marioli, A. Taroni, Characterization of Thermoelectric Modules for Powering Autonomous Sensors, IEEE Trans. on Instrumetation and Measurement, vol. 58, April 2009, pp. 99-107.

[14] D. Yang, H. Yin, Energy Conversion Efficiency of a Novel Hybrid Solar System for Photovoltaic, Thermoelectric and Heat Utilization, IEEE Transaction on Energy Conversion, vol. 26, September 2011, pp. 662-670.

[15] S. Dalola, V. Ferrari, M. Guizzetti, D. Marioli, E. Sardini, M. Serpelloni, A. Taroni, Autonomous Sensor System with Power Harvesting for Telemetric Temperature Measurements od Pipes, IEEE Transactions on Instrumentation and Measurement, vol.58, no. 5, May 2009, pp.1 471-1478.

[16] M. Chen, Distributed Detection and Control of Defective Thermoelectric Generation Modules Using Sensor Nodes, IEEE Transactions on Instrumentation and Measurement, vol.63, no. 1, Jannuary 2014, pp.192-202.

[17] W. He, J. Zhou, C. Chen, J. Ji, Experimental study and performance analysis of a thermoelectric cooling and heating system driven by a photovoltaic/thermal system in summer and winter operation modes, Energy Conversion and Management, n. 84, August 2014, pp. 41-49.

[18] M. Herrando, C. N. Markides, K. Hellgardt, A UK-based assessment of hybrid PV and solar-thermal systems for domestic heating and power: System performance, Applied Energy, n. 122, June 2014, pp 288-309 .

[19] J.- A. Jiang, Y. L. Su, J. C. Shieh, K. C. Kuo, T. S. L. T. T. Lin, W. Fang, J. J. Chou, J. C. Wang, On application of a new hybrid maximum power point tracking (MPPT) based photovoltaic system to the closed plant factory, Applied Energy, n. 124, n. 1, July 2014, pp. 309-324.

[20] D. Kamthania, G.N. Tiwari, Energy metrics analysis of semi-transparent hybrid PVT double pass facade considering various silicon and non-silicon based PV module Hyphen Solar Energy, n. 100, February 2014, pp. 124-140.

[21] H. Chen, N. Wang, H. He, Equivalent Circuit Analysis of Photovoltaic-Thermoelectric Hybrid Device with Different TE Module Structure, Advances in Condensed Matter Physics, n. 2014, May 2014, pp. 1-6.

[22] G. Andria, A M.L. Lanzolla, F. Piccininni, G. S. Virk , Design and Characterization of Solar Assisted Heating Plant in Domestic Houses, IEEE Transactions on Instrumentation and Measurement, vol. 57, no. 12, December 2008, pp. 2711-2719.

[23] H. A. Zondag, Flat-plate PV-Thermal Collectors and Systems: a Review, Renewable Sustainable Energy, vol. 12, May 2008, pp. 1-16.

[24] D. Mitrani, J. A. Tomé, J. Salazar, A. Turò, Methodology for Extracting Thermoelectric Module Parameters, vol. 54, August 2005, pp. 1548-1552.

[25] W. G. J. H. M. van Sark, Feasibility of Photovoltaic - Thermoelectric hybrid Modules, Applied Energy, vol. 88, August 2011, pp. 2785-2790.

[26] S. LeBlanc, S. K. Yee, M. L. Scullin, C. Damesd, K. E. Goodson, Material and manufacturing cost considerations for thermoelectrics, Renewable and Sustainable Energy Reviews, n. 32 , April 2014, pp.313–327.

[27] X. Zhang, K. T. Chau, C. C. Chan, S. Gao, An Automotive Thermoelectric-Photovoltaic Hybrid Energy System, Proc. of IEEE Vehicle Power and Propulsion Conference, Lille, France, September, 2010, pp. 1-5.

[28] W. Roth, R. Kugele, A. Steinhoser, W. Schulz, G. Hille, Grid-independent power supply for repeaters in mobile radio networks using photovoltaic-thermoelectric hybrid systems, Proc. of Thermoelectrics International Conference, Cardiff, Wales, September 1997, pp. 582-585.

[29] N. Smith, R. Mc Cann, Investigation of a Multiple Input Converter for Grid Connected Thermoelectric-Photovoltaic Hybrid System, Proc. of IEEE Green Technologies Conference, Tulsa, USA, April 2012, pp. 1-5.

[30] Y. Fan, L. Ge, W. Hua, Multiple-input DC-DC Converter for the Thermoelectric-Photovoltaic Energy System, Proc. of IEEE Vehicle Power and Propulsion Conference, Lille, France, September, 2010, pp. 6-10.

[31] Photovoltaic Geographical Information System (PVGIS), http://re.jrc.ec.europa.eu/pvgis/

[32] A. Drews, A. C. de Keizer, H. G. Beyer, Monitoring and Remote Failure Detection of Grid-Connected, Solar Energy, vol. 81, September 2007, pp. 548-564.

[33] M. R. Al Rashidi, M. F. Al Hajri, K. M. El-Naggar, A. K. Al-Othman, A New Estimation Approach for Determining the I–V Characteristics of Solar Cells, Solar Energy, July 2011, vol. 85, pp. 1543-1550.

[34] A. Goetzberger, V. U, Hoffmann, Photovoltaic Solar Energy Generation, Spingler-Verlag, 2005.

[35] F. Adamo, F. Attivissimo, A. Di Nisio, M. Spadavecchia, Characterization and Testing of a Tool for Photovoltaic Panel Modeling, IEEE Trans. on Instrum. Meas., April 2011, vol. 60, pp. 1613-1622.

[36] F. Attivissimo, A. Di Nisio, M. Savino, M. Spadavecchia, Uncertainty analysis in photovoltaic cell parameters estimation, IEEE Trans. on Instrum. Meas., April 2012, vol. 61, pp. 1334-1342.

[37] F. Adamo, F. Attivissimo, A. Carullo, A. M. L. Lanzolla, F. Spertino, A. Vallan, On the Performance of the Double-diode Model in Estimating the Maximum Power Point for Different Photovoltaic Techonologies, Measurement, June 2013, vol. 46, pp. 3549-3559.

[38] F. Attivissimo, D. Passaghe, A. M. L. Lanzolla, M. Paul, D. Gregory, A. Knox, Photovoltaic-Thermoelectric modules: a feasibility study, Proc.of I2MTC/14, Montevideo, Uruguay, May 2014, pp. 659-664.

[39] J. Gao, M. Chen, Beat the Deviation in Estimating Maximum Power of Thermoelectric Modules, IEEE Transactions on Instrumentation and Measurement, vol. 62, no. 10, October 2013, pp. 2725-2729.

[40] D. Rowe, CRC Handbook of Thermoelectrics, CRC , 1995.

[41] J. L. Bierscheck, D. A. Johson, Latest Developments in Thermoelectrically Enhanced Heat Sink, August 2005, vol. 11, pp. 659-664.

[42] G. Casano, S. Piva, Experimental Investigation of the Performance of a Thermoelectric Generator based on Peltier Cells, October 2011, vol. 35, pp. 660-669.

[43] https://home.zhaw.ch/~fusa/PSS_VLE_C/CHAPTER_03/CASES/Materials/CP2-127-06L.pdf

[44] N. Le Pierres, M. Cosnier, L. Luo, G. Fraisse, Coupling of Thermoelectric modules with a Photovoltaic Panel for Air Preheating and precooling application: an annual simulation, Journal of Energy Research, July 2008, vol. 32, pp. 1316-1328.

[45] S. B. Riffat, X. Ma, R. Wilson, Performance Simulation and Experimental Testing of a Novel Thermoelectric Heat Pump System, Applied Thermal Engineering, October 2006, vol. 26, pp. 494-501.

[46] N. Wang, L. Han, H. He, N. H. Park, K. Koumoto, A Novel High-performance Photovoltaic-thermoelectric Hybrid Device, Energy and Environmental Science, vol. 9, no. 4, August 2011, pp. 3676-3679.

[47] E. A. Chavez-Urbiola, Y. V. Vorobiev, L. P. Bulat, Solar Hybrid Systems with Thermoelectric Generators, Solar Energy, vol. 86, September 2012, pp. 369-378.

[48] L. Cristaldi, M. Faifer, M. Rossi, S, Toscani, An Improved Model-Based Maximum Power Point Tracker for Photovoltaic Panels, IEEE Trans. on Instrum. Meas., Jannuary 2014, vol 63, pp. 63-71.

[49] D. M. Rowe, G. Min, Evaluation of Thermoelectric Modules for Power Generation, Journal of Power Sources, June 1998, vol. 73, pp. 193-198.

[50] IEC, Photovoltaic System Performance Monitoring - Guidelines for Measurement, data exchange and Analysis, IEC Standard 61724, Geneva, Switzerland, 1998.

[51] National Renewable Energy Laboratory (SOLPOS), http://www.nrel.gov/midc/

[52] E. Skoplaki, J. A. Palyvos, Operating Temperature of photovoltaic modules: A survey of pertinent correlations, Renewable Energy, June 2009, vol. 34, pp. 23-29.

[53] www.istarsolar.com/upload/imagefile/pdf/moduli/poly/is10P-is20P-is30P-is45P-is50P_IT_513.pdf

[54] www.eureca.de/english/cooling_teg_kryotherm.html

[55] /www.ecobusinesslinks.com/surveys/free-solar-panel-price-survey